8592 *Biochemistry* **2010,** *49,* 8592–8598
DOI: 10.1021/bi1004377

BIOCHEMISTRY
including biophysical chemistry & molecular biology
Article

Topology of Transmembrane Channel-like Gene 1 Protein†

Valentina Labay, Rachel M. Weichert, Tomoko Makishima, and Andrew J. Griffith*

Molecular Biology and Genetics Section, Otolaryngology Branch, National Institute on Deafness and Other Communication Disorders, National Institutes of Health, Rockville, Maryland 20850

Received March 23, 2010; Revised Manuscript Received July 28, 2010

ABSTRACT: Mutations of transmembrane channel-like gene 1 (*TMC1*) cause hearing loss in humans and mice. *TMC1* is the founding member of a family of genes encoding proteins of unknown function that are predicted to contain multiple transmembrane domains. The goal of our study was to define the topology of mouse TMC1 expressed heterologously in tissue culture cells. TMC1 was retained in the endoplasmic reticulum (ER) membrane of five tissue culture cell lines that we tested. We used anti-TMC1 and anti-HA antibodies to probe the topologic orientation of three native epitopes and seven HA epitope tags along full-length TMC1 after selective or complete permeabilization of transfected cells with digitonin or Triton X-100, respectively. TMC1 was present within the ER as an integral membrane protein containing six transmembrane domains and cytosolic N- and C-termini. There is a large cytoplasmic loop, between the fourth and fifth transmembrane domains, with two highly conserved hydrophobic regions that might associate with or penetrate, but do not span, the plasma membrane. Our study is the first to demonstrate that TMC1 is a transmembrane protein. The topologic organization revealed by this study shares some features with that of the shaker-TRP superfamily of ion channels.

Mutations in transmembrane channel-like gene 1 (*TMC1*/*Tmc1*) can cause dominant or recessive hearing loss in humans and mice (*1*, *2*). *Tmc1* mRNA is specifically expressed in neurosensory hair cells of the inner ear (*1*, *2*). Cochlear neurosensory hair cells of *Tmc1* mutant mice fail to mature into fully functional sensory receptors (*3*) and exhibit concomitant structural degeneration that could be a cause or an effect of the maturational defect (*2*). The molecular and cellular functions of TMC1[1] protein remain unknown due, at least in part, to in situ expression levels that are prohibitively low for direct biochemical analysis.

There are seven additional mammalian TMC paralogs whose structure and function are also unknown. There are no significant sequence similarities between any TMC protein and other proteins of known function. An initial PSORT-II analysis of human and mouse TMC proteins did not detect any N-terminal signal sequences or other trafficking signals, but it did predict that TMC proteins reside in the plasma membrane (*4*). The TMC proteins are all predicted to contain 6−10 transmembrane domains (TMDs) and a novel, conserved region, which we termed the TMC domain (*4*). TMHMM2.0 analysis of mouse and human TMC1 predicts cytoplasmically oriented N- and C-termini and six TMDs that are also predicted for the other paralogs (*4*). Other algorithms such as PSORT-II and TopPred predict two to four additional TMDs, for a total of 8−10 TMDs, per TMC homologue (*2*, *5*). PROSITE and NetNGlyc identified several TMC sequence sites with varying probabilities of glycosylation, but neither PSORT-II nor SignalP detected an N-terminal signal peptide sequence (*4*). The in situ cellular location of TMC proteins is unknown, but human TMC6 (also known as EVER1) and TMC8 (EVER2) proteins expressed in transiently transfected human HaCaT keratinocyte cells appear to be retained in the endoplasmic reticulum (*6*). Truncating mutations of *EVER1* and *EVER2* cause epidermodysplasia verruciformis (EV; MIM 226400), characterized by susceptibility to cutaneous human papilloma virus infections and associated non-melanoma skin cancers (*6*).

The purpose of our study was to determine the transmembrane topology of TMC1. We performed our experiments on mouse TMC1 (mTMC1) expressed in transiently transfected COS-7 and HeLa cells. We used differential detergent treatment to distinguish cytoplasmic from intraluminal epitopes of transmembrane proteins in the endoplasmic reticulum (ER). Our results indicate that heterologously expressed mTMC1 is an integral membrane protein with six TMDs and cytoplasmically oriented N- and C-termini.

EXPERIMENTAL PROCEDURES

Antibodies. We derived polyclonal antisera 272, 277, 274, and 255 from rabbits immunized with keyhole limpet hemocyanin (KLH)-conjugated synthetic peptides corresponding to mTMC1 amino acids 21−39 (EEDKLPRRESLRPKRKRTR), 53−72 (DEETRKAREKERRRRLRRGA), 216−236 (GSLPRKTVPRAEEASAANFGV), and 731−747 (MKQQALENKMRNKKMAA), respectively. We ordered peptides from Princeton BioMolecules (Langhorne, PA) and antibodies from Covance Research Products (Denver, PA). We purchased polyclonal anti-β-tubulin and monoclonal anti-PDI (Abcam, Cambridge, MA), monoclonal anti-α-tubulin (Molecular Probes, Carlsbad, CA), polyclonal anti-GRP94, and monoclonal anti-KDEL (Stressgen, San Diego, CA). Monoclonal anti-hemagglutinin (HA) antibodies were from Abcam and polyclonal anti-HA antibodies from Covance.

†This work was supported by National Institutes of Health Intramural Research Fund Z01-DC-000060.

*To whom correspondence should be addressed: 5 Research Ct., Room 2B28, Rockville, MD 20850. Telephone: (301) 496-1960. Fax: (301) 402-7580. E-mail: griffita@nidcd.nih.gov.

[1]Abbreviations: ER, endoplasmic reticulum; TMC1, transmembrane channel-like gene 1 protein product; TMD, transmembrane domain; mTMC1, mouse TMC1; KLH, keyhole limpet hemocyanin; KDEL, amino acid sequence of an ER retention signal; PVDF, polyvinylidene fluoride.

 Published on Web 08/02/2010

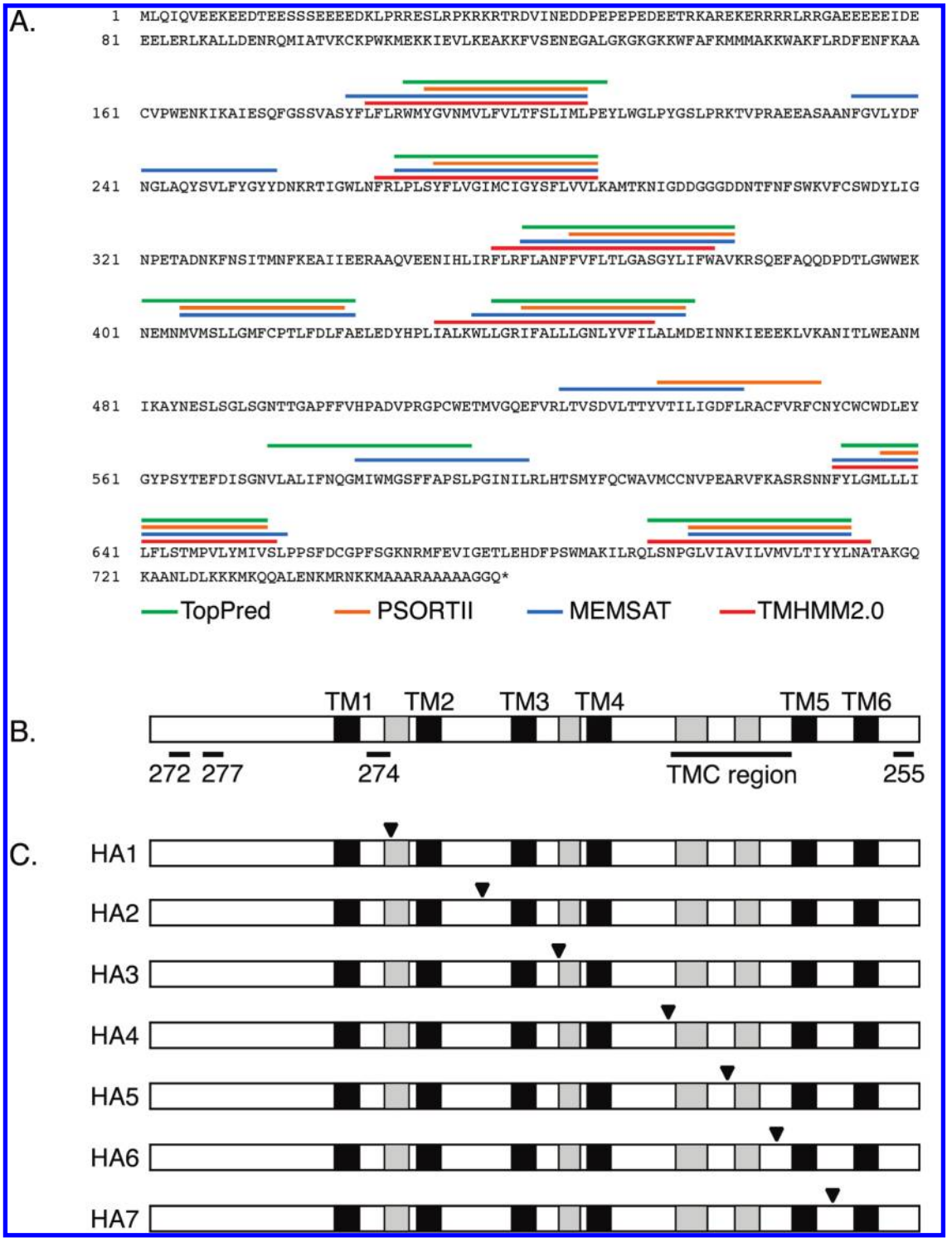

FIGURE 1: Potential models of membrane topology, immunogenic peptides, and epitope tags of mTMC1. (A) Deduced amino acid sequence of mTMC1 and transmembrane domains predicted by TMHMM2.0 [red (*17*)], MEMSAT [blue (*27*)], PSORT-II [orange (*28*)], and TopPred [green (*29*)]. Each algorithm used standard parameters for eukaryotic membrane proteins. (B) Schematic illustration of mTMC1 showing six regions (black for TM1−TM6) with hydropathy values higher than 1.6 and four regions (gray) with hydropathy values between zero and 1.6. Also shown are the positions of the TMC domain and of the four synthetic peptides used to generate anti-TMC1 antisera 272, 274, 277, and 255. (C) Schematic illustration of HA-tagged mTMC1 expression constructs with tag insertion positions (black triangles).

Plasmids. We PCR-amplified the full-length mouse *Tmc1* open reading frame from a previously reported cDNA clone in pGEM T-easy (*1*). Our sense (5′-GCT AGC ATG TTG CAA ATC CAA GTG-3′) and antisense (5′-GGA TCC CTG GCC ACC AGC AGC TGC-3′) amplification primers contained NheI and BamHI restriction sites, respectively, for subsequent cloning. We used site-directed mutagenesis (QuickChange, Stratagene, La Jolla, CA) to insert one HA epitope tag (YPYDVPDYA) (*7*) per expression construct at each of seven sites. Each pair of 67 bp mutagenic primers contained 27 bp (5′-TAC CCA TAT GAC GTC CCG GAC TAC GCC-3′) encoding the HA tag, flanked by two 20 bp *Tmc1* sequences encoding each side of the target insertion site. The HA tag was inserted between amino acids 237 and 238 (HA1), 327 and 328 (HA2), 402 and 403 (HA3), 510 and

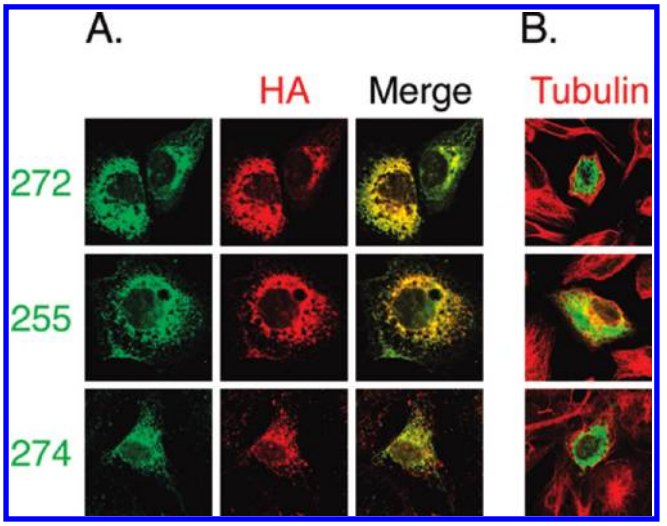

FIGURE 2: Specificity of mTMC1 antibodies. COS-7 cells were transfected with HA-tagged mTMC1 (construct HA2) and costained with either anti-HA or anti-tubulin antibody and each of three different anti-TMC1 antisera. (A) Immunoreactivity with anti-TMC1 antiserum 272, 255, or 274 (green) (left column). Immunoreactivity with anti-HA antibody (red) (middle column). Merge of left and middle panels (right column). Immunoreactivity with anti-HA completely overlaps with that of each of the different anti-TMC1 antibodies. (B) Merge of anti-tubulin (red) immunoreactivity used to visualize all cells and antiserum 272, 255, or 274 (green) immunoreactivity. Anti-TMC1 immunoreactivity is seen only in transfected cells.

511 (HA4), 568 and 569 (HA5), 616 and 617 (HA6), and 671 and 672 (HA7) (Figure 1C). Clones were sequenced, to verify correct insertion of the HA tag sequence without unwanted mutagenic events, and digested with NheI and BamHI. The cDNA inserts were purified by 1% agarose gel electrophoresis and QIAquick gel extraction (Qiagen, Valencia, CA) and subcloned into NheI- and BamHI-digested pcDNA3.1(−) (Invitrogen, Carlsbad, CA).

Tissue Culture and Transient Transfection. COS-7 and HeLa cells were grown in DMEM (Invitrogen) with 10% fetal bovine serum in an incubator at 37 °C with 5% CO_2. For immunofluorescence assays, cells were grown on glass coverslips in six-well plates (Corning Glass, Lowell, MA) and transfected with the expression construct using Lipofectamine 2000 (Invitrogen) for COS-7 cells or FuGENE HD (Roche, Indianapolis, IN) for HeLa cells. COS-7 and HeLa cells were incubated in the transfection mix in a 5% CO_2 incubator at 37 °C for 18−24 h. Cells were grown in T75 flasks (Corning Glass) and incubated with transfection mix for 18−24 h for protein extraction.

Protein Extraction. Transiently transfected cells were detached with PBS containing 1 mM EDTA for 5−10 min at 37 °C. All of the following procedures were conducted on ice or at 4 °C. Cells were washed twice in PBS, resuspended in MB buffer [210 mM mannitol, 70 mM sucrose, 1 mM EGTA, and 10 mM Hepes (pH 7.5), protease inhibitor cocktail III (Calbiochem, Gibbstown, NJ)], and incubated for 1 h. Cells were lysed by 20 passages through a 29 gauge × 1/2 in. (0.34 mm × 13 mm) needle on a 1 mL syringe (Kendall, Tyco Healthcare Group, Mansfield, MA). Microscopic examination assured that cell lysis was 99% complete. The lysed cell suspension was centrifuged at 600*g* for 10 min to pellet the nuclei. The supernatant was regarded as a whole cell lysate. Microsomes were prepared by a 20 min centrifugation of the whole cell lysate at 6800*g* to remove mitochondria. The resulting supernatant was centrifuged for 1 h at 100000*g* to produce a microsomal pellet, which was resuspended in MB buffer.

Western Blot Analysis. Whole cell extracts and microsomal preparations were denatured when they were boiled in NuPAGE LDS sample buffer (Invitrogen) for 5 min. Samples were separated by SDS−PAGE on 4 to 12% Bis-Tris gels using either MOPS or MES buffer (Invitrogen). Proteins were transferred to PVDF membranes (Millipore, Billerica, MA), blocked overnight with 5% nonfat dry milk in TBST [10 mM Tris-HCl (pH 7.5), 150 mM NaCl, and 0.05% Tween 20], and probed with either anti-TMC1 antibody 277 or polyclonal anti-HA antibody (both at a 1:400 dilution). Proteins were detected by ECL using a 1:10000 dilution of horseradish peroxidase-conjugated anti-rabbit IgG (Amersham, Piscataway, NJ) or with the Typhoon Trio Plus imaging system (GE Healthcare Life Sciences, Piscataway, NJ) using a 1:2500 dilution of ECL Plex Cy5 fluorescent anti-rabbit secondary antibody (Amersham).

Immunofluorescence. All procedures were performed at room temperature. Cells on coverslips were washed three times with PBS, fixed with 4% paraformaldehyde in PBS for 10 min, and washed again three times with PBS for 10 min each. The plasma membrane was selectively permeabilized with 5 μg/mL (0.0005%) digitonin (Sigma, St. Louis, MO) in incubation buffer [0.3 M sucrose, 2.5 mM $MgCl_2$, 0.1 M KCl, 1 mM EDTA, and 10 mM Pipes (pH 6.8)] for 4 min. Alternatively, permeabilization of the plasma and ER membranes was achieved by incubation with 0.25% Triton X-100 in PBS for 10 min. Immediately following permeabilization, cells were washed three times with PBS and blocked with 2% bovine serum albumin (Roche) and 5% goat serum (Invitrogen) in PBS for 30 min. Cells were then incubated for 1 h with primary antibodies: polyclonal antiserum 272, 255, or 274 or a monoclonal antibody to hemagglutinin. Cells were costained with antibodies to cytosolic tubulin, and ER luminal protein PDI or GRP94 or soluble ER resident proteins carrying the KDEL retention signal. We initially used an anti-PDI antibody to stain COS-7 cells, but it produced strong background staining with HeLa cells. We also tried antibodies against KDEL and GRP94 and found that anti-GRP94 gave the best results with HeLa cells. Cells were washed three times with PBS and incubated with secondary antibodies (Alexa Fluor, Invitrogen) for 30 min. After three 15 min washes with PBS, we mounted the coverslips onto glass slides and added ProLong Gold antifade reagent (Invitrogen). We randomly chose approximately 20−30 different areas of each sample for visualization with a Zeiss LSM510 confocal microscope, a 63× apochromat oil immersion phase-contrast objective, and Texas Red or FITC optics.

RESULTS

Potential mTMC1 Transmembrane Topologic Models. We compared the topologies of mTMC1 predicted by four different algorithms (Figure 1A). Although the number of predicted TMDs varies among algorithms, all of the algorithms predicted the N-terminus of mTMC1 to be cytoplasmic. A Kyte−Doolittle hydropathy plot detects 10 hydrophobic regions, including six regions with a hydropathy score of >1.6 (Figure 1B) and, thus, a higher probability of spanning the membrane (*8*). The latter six regions are predicted to be TMDs by all of the algorithms, whereas the four regions with lower hydropathy scores are predicted to be TMDs by only some of the algorithms (Figure 1A,B).

Validation of mTMC1 Antibodies. We tested the specificity of mTMC1 antibodies 272, 274, and 255 in immunofluorescence staining. We expressed HA epitope-tagged mTMC1 (construct

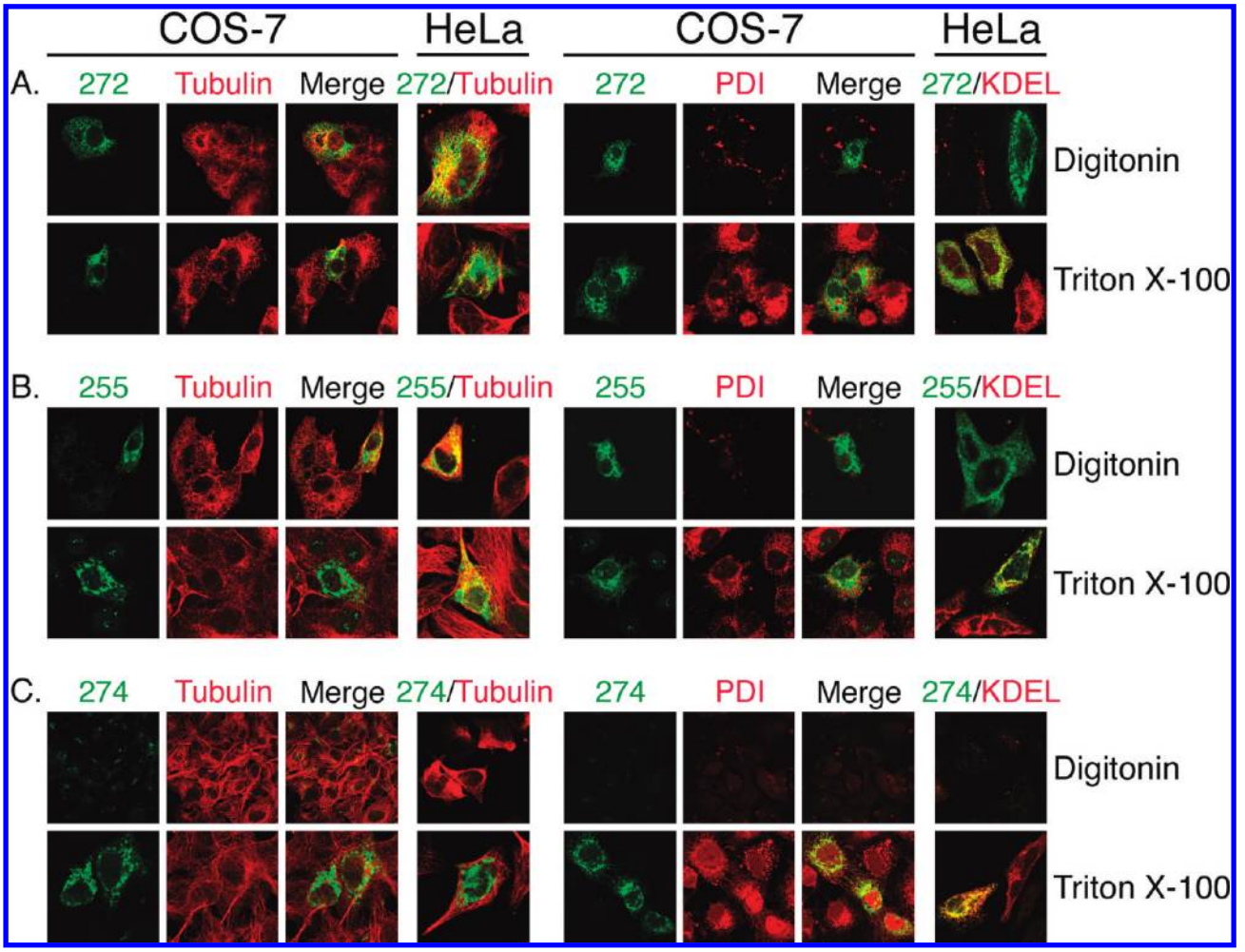

FIGURE 3: Topology probed by mTMC1 epitope accessibility. COS-7 or HeLa cells transfected with native mTMC1 were either selectively or fully permeabilized with digitonin or Triton X-100, respectively. Cells were stained with each of the anti-TMC1 antisera as well as antibodies against ER luminal protein PDI or soluble ER resident proteins carrying the KDEL retention signal (right panels) or cytosolic tubulin (left panels) to evaluate the extent of permeabilization. Only merged images are shown for HeLa cells as similar results were obtained for both cell lines. (A and B) N- and C-terminal epitopes (recognized by antisera 272 and 255, respectively) and tubulin are readily detected following digitonin permeabilization (top rows), whereas PDI and KDEL are only accessible following full permeabilization by Triton X-100 (bottom rows). (C) PDI and KDEL and the epitope recognized by antiserum 274 are only accessible after Triton X-100 permeabilization (bottom row).

HA2) in COS-7 cells. Cells were permeabilized with Triton X-100 and costained with anti-HA antibody and one of each of the three anti-TMC1 antisera (Figure 2A), or costained with anti-tubulin and one of each of the anti-TMC1 antisera (Figure 2B). Immunoreactivity with anti-HA completely overlaps with that of each of the anti-TMC1 antibodies, confirming that the TMC1 antibodies specifically recognize TMC1 in this assay (Figure 2A). Immunoreactivity with anti-TMC1 antibody is only detected in transfected cells, further validating the specificity of anti-TMC1 antibodies in this assay (Figure 2B).

Heterologous Expression and Localization of mTMC1. We repeated the PSORT-II analysis of TMC proteins. The results indicate that all human and mouse TMC proteins might reside in the ER membrane, albeit at a lower probability (18−39%) than in the plasma membrane (56−72%). Immunofluorescence analysis of epitope-tagged mTMC1 expressed in a variety of different tissue culture cell lines (COS-7, HeLa, SHSY5Y, HEK293, and MDCK) results in a reticular pattern consistent with the location of the ER and overlapping with staining for ER-specific proteins (Figures 3 and 5). We could not detect plasma membrane localization by staining unfixed, nonpermeabilized tissue culture cells expressing mTMC1 (results not shown). In contrast, other multipass transmembrane proteins (TRPV4 and pendrin) traffic normally to the plasma membrane in this expression system (*9*). We identified several known (amino acids 35−37 and 64−67) as well as putative (amino acids 37−39 and 67−69) arginine-based ER retention signals of the RXR type (*10*−*12*) in the N-terminal region of mTMC1. Disrupting these retention signals by alanine mutagenesis does not affect ER retention (results not shown).

While the ER could be the in situ location of mTMC1, our results may also reflect retention of overexpressed and misfolded mTMC1 in the ER, a lack of appropriate trafficking signals or partners to deliver mTMC1 to the plasma membrane, or a combination of these mechanisms.

Topologic Structure Determined by Native mTMC1 Epitope Accessibility. We used polyclonal antisera 272, 255, and 274 to determine the epitope accessibility, and thus topologic orientation, of amino acids 21−39 in the N-terminus, amino acids 731−747 in the C-terminus, and amino acids 216−236 in the first predicted internal loop, respectively, in native mTMC1 protein (Figure 1B). We either permeabilized all plasma and intracellular membranes with 0.25% Triton X-100 or selectively permeabilized only the plasma membrane while leaving the ER membrane intact with 5 μg/mL digitonin (*13*, *14*). We used

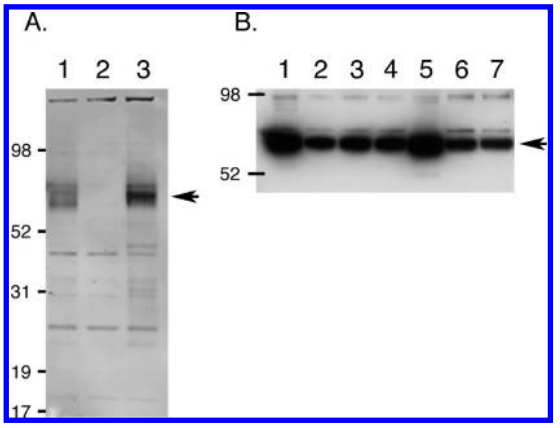

FIGURE 4: Western blot analysis of native and HA-tagged mTMC1. (A) Whole cell lysates of COS-7 cells transiently transfected with a native mTMC1 expression construct (lane 1), empty pcDNA3.1(−) vector (lane 2), and a representative HA (HA4) expression construct (lane 3) were resolved on a 4 to 12% Bis-Tris gel using MOPS running buffer. The immunoblot was probed with anti-TMC1 antibody 277. An arrow indicates a strong band of the expected size (approximately 87 kDa) in lanes 1 and 3, but not in lane 2. (B) Microsomal extractions from COS-7 cells transiently transfected with each of the HA-tagged constructs HA1−HA7 (lanes 1−7, respectively) were resolved on a 4 to 12% Bis-Tris gel using MES running buffer. The blot was probed with anti-HA antibody. The arrow indicates a band of the expected size in all lanes.

antibodies against ER luminal protein PDI or soluble ER resident proteins carrying the KDEL retention signal, or against cytosolic tubulin to evaluate the extent of permeabilization. The native mTMC1 N- and C-terminal epitopes and tubulin were accessible for binding to their respective antibodies with either Triton X-100 or digitonin permeabilization of either COS-7 or HeLa cells (Figure 3A,B). In contrast, amino acids 216−236 of mTMC1, and the ER luminal proteins, were accessible to antibodies only when cells were exposed to Triton X-100 (Figure 3C). These results demonstrate that the N- and C-termini of native mTMC1 are oriented toward the cytoplasm and the predicted first internal loop is oriented toward the ER lumen.

mTMC1 Topology Determined by HA Epitope Accessibility. We designed a series of HA-tagged *mTMC1* expression constructs to differentiate among the possible mTMC1 topological models (Figure 1C). The topologic orientations of tagged regions were determined by their accessibility to anti-HA antibodies after differential detergent treatment. The insertion of the nine-amino acid HA tag into hydrophilic loops of other proteins typically has little or no effect on their structure and function (*15*, *16*). The HA-tagged constructs were transiently expressed in either HeLa or COS-7 cells to yield HA-tagged mTMC1 proteins of the predicted size (Figure 4).

The HA epitopes encoded by HA1, HA3, and HA7 and the ER luminal protein GRP94 were accessible to antibodies only after permeabilization with 0.25% Triton X-100 (Figure 5). These results demonstrate that the TMHMM2.0-predicted first, third, and fifth loops of mTMC1 flanked by transmembrane domains TM1 and TM2, TM3 and TM4, and TM5 and TM6, respectively, are all oriented toward the ER lumen. In contrast, the HA epitope encoded by HA2 and the cytosolic marker tubulin were accessible for antibody binding after either Triton X-100 or digitonin treatment (Figure 5).

The TMHMM2.0-predicted loop flanked by TM4 and TM5 contains a region of hydrophobic residues predicted by other algorithms (MEMSAT, PSORT-II, and TopPred) to include one or

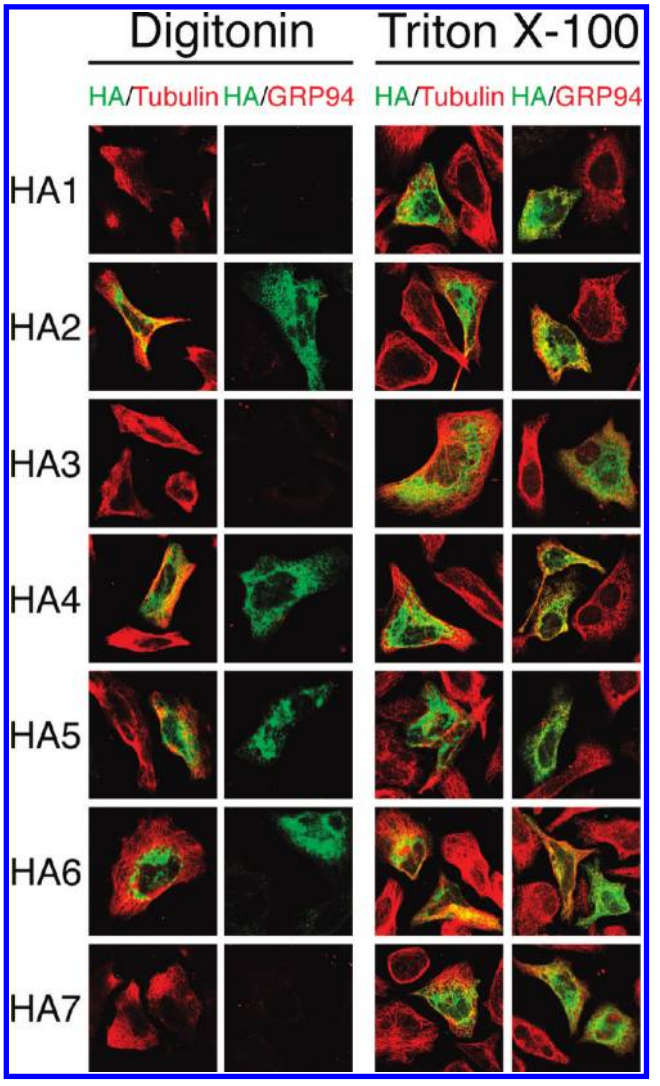

FIGURE 5: Topology probed by HA epitope tag accessibility. HeLa cells transfected with each of the HA-tagged mTMC1 expression constructs were permeabilized with either digitonin (left panels) or Triton X-100 (right panels). With each treatment, cells were costained with anti-HA (green) and anti-tubulin (red) antibodies or with anti-HA (green) and anti-GRP94 (red) antibodies. Tubulin and the HA epitope tags of HA2 and HA4−HA6 were accessible to antibodies after selective permeabilization with digitonin. In contrast, GRP94 and the HA epitope tags of HA1, HA3, and HA7 were stained only after full permeabilization with Triton X-100.

two additional TMDs (Figure 1A,B). We designed and expressed constructs HA4−HA6 to differentiate among these models. Their HA epitopes as well as tubulin were stained by antibodies after either Triton X-100 or digitonin treatment, whereas GRP94 was stained only after Triton X-100 (Figure 5). These results confirm that all three HA epitope tags inserted into the loop flanked by TM4 and TM5 are oriented toward the cytoplasm.

The topologic orientations of the HA epitopes in the seven different HA-tagged mTMC1 expression constructs confirm the TMHMM2.0-predicted model of six membrane-spanning domains and rule out the existence of the additional TMDs predicted by other algorithms. The accessibility of the HA epitope tag encoded by HA1 only after Triton X-100 permeabilization is consistent with the result with native mTMC1 and antibody 274. This indicates that the insertion of the HA tag into the TMHMM2.0-predicted first loop of mTMC1 had no effect on its orientation. Furthermore, the insertion of HA epitope tags did

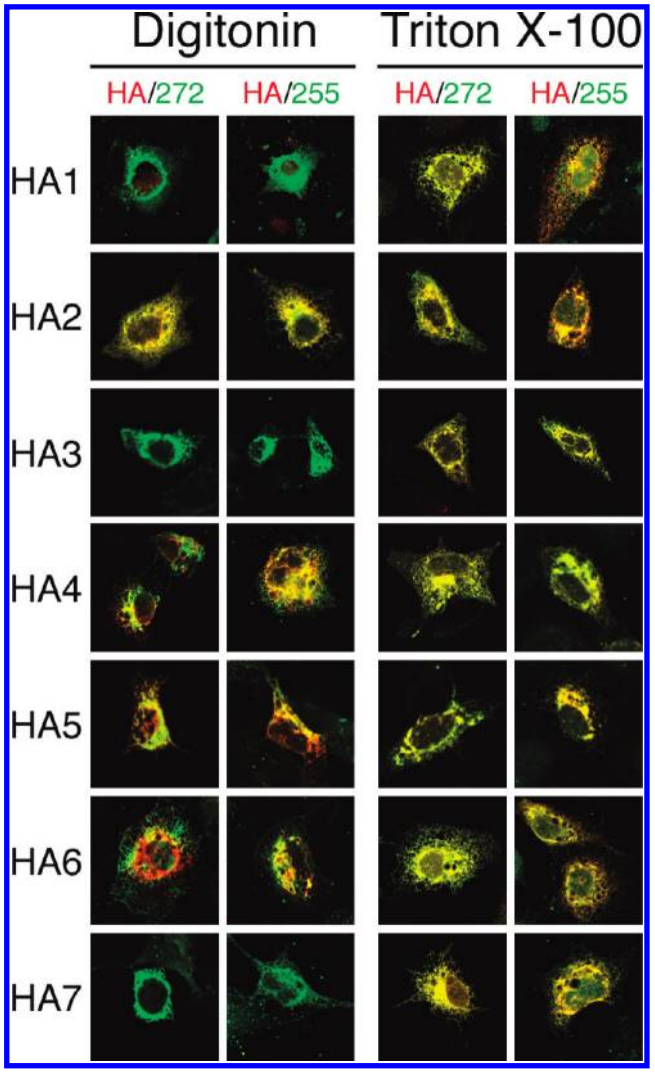

FIGURE 6: Preservation of N- and C-terminal topology in HA epitope-tagged mTMC1. COS-7 cells transfected with each of the HA-tagged mTMC1 expression constructs were permeabilized with either digitonin (left panels) or Triton X-100 (right panels). Cells were stained with anti-HA antibody (red) and with antiserum 272 or 255 (green). The N- and C-terminal epitopes of each expression product are accessible for staining with their respective antibodies following digitonin permeabilization. Anti-TMC1 staining of HA1, HA3, and HA7 appears green because the HA tags inserted in the internal loops are not accessible for staining. For HA2 and HA4−HA6, the HA tag is inserted in an accessible cytoplasmic loop and its (red) staining overlaps the green staining of N- and C-terminal epitopes and appears yellow.

not disrupt the cytoplasmic orientation of the N- and C-termini that was observed for both the HA-tagged expression constructs and native mTMC1 (Figure 6).

DISCUSSION

In this study, we investigated the topological organization of mTMC1 heterologously expressed in COS-7 or HeLa cells. The reticular expression pattern of heterologous mTMC1 indicates that it was localized within or associated with the endoplasmic reticulum membranes. TMHMM2.0 was previously reported to be the best-performing topology prediction algorithm (*17*−*19*). Our results are consistent only with the TMHMM2.0-predicted model of mTMC1 having cytoplasmically oriented N- and C-termini and six transmembrane domains (Figure 7).

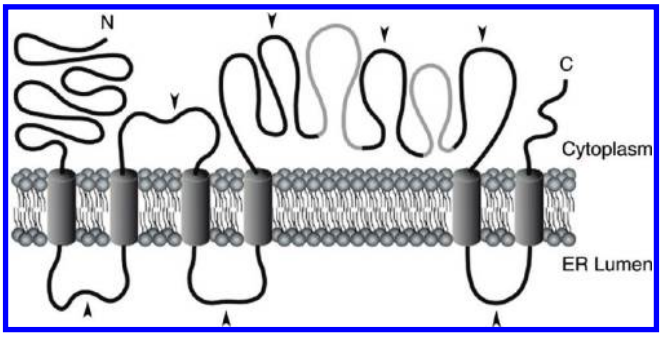

FIGURE 7: Model for the membrane topology of mTMC1. Our results show that mTMC1 expressed in COS-7 or HeLa cells contains six membrane-spanning domains with N- and C-termini oriented toward the cytoplasm. The model is shown with TM4 and TM5 flanking a long cytoplasmic loop. The two gray regions in this loop are predicted to be TM domains at very low probability and might be membrane-associated or re-entrant domains. Black arrowheads indicate HA tag insertion sites.

Although some algorithms predict the existence of additional TMDs in mTMC1 and other TMC proteins, only the domains homologous to the six TMDs of mTMC1 are predicted to span membranes by all algorithms. Furthermore, in silico hydrophobicity analyses of other TMC proteins indicate that these homologous domains consistently have the highest hydropathy values (>1.6). The six-pass transmembrane topology of mTMC1 may therefore be a shared structure with all TMC proteins.

The large cytoplasmic loop flanked by TM4 and TM5 includes the TMC domain (Figure 1B), which is highly conserved among all TMC proteins, including TMC homologues in *Drosophila melanogaster* and *Caenorhabditis elegans* (*4*). Although the function of this region is unknown, its importance is highlighted by an in-frame deletion of 57 amino acids of the large cytoplasmic loop, including part of the TMC domain, encoded by the *Tmc1*^{dn} allele of the deafness (*dn*) mutant mouse strain (*1*). This region contains eight cysteine residues, including at least three (amino acids 553, 555, and 610) that are highly conserved and one (amino acid 512) that is conserved among all known TMC homologues (*4*, *5*). These residues are likely to be required for TMC1 function and structure and thus may confound a cysteine accessibility approach to probe the topology of this region in the absence of a functional assay to rule out misfolding. The TMC domain also contains two mildly hydrophobic regions that are predicted, at low probability, to span the membrane by some algorithms, but not by TMHMM2.0 (Figure 7). Because the three HA epitope tags flanking these regions of mTMC1 were all oriented toward the cytoplasm (Figures 5 and 7), these two segments might be membrane-associated or re-entrant domains. This raises the possibility that these mildly hydrophobic segments contribute to a pore-forming structure of TMC1 if it is a channel or transporter. Indeed, ProtFun 2.2 (*20*, *21*) predicts that all human and mouse TMC proteins are transporters or, at a lower probability, ion channels.

We do not have a functional assay for TMC1, and we cannot rule out the possibility that mTMC1 expression products are retained in the ER due to incomplete folding or misfolding. Polytopic membrane proteins depend on specialized membrane-localized chaperones to prevent inappropriate interactions between membrane-spanning segments as they insert and fold in the ER membrane (*22*). In the absence of these chaperones, membrane proteins are retained in the ER despite correct insertion of

their membrane-spanning segments. A lack of hair cell-specific chaperones, trafficking signals, or protein partners in our heterologous expression systems could also lead to ER retention of properly folded TMC1 protein.

The topology of mTMC1 resembles that of a large superfamily of proteins that includes TRP channels and voltage-gated K channels. These proteins also have six membrane-spanning segments (S1−S6) and cytoplasmic N- and C-termini (*23*, *24*). However, we cannot detect any specific sequence similarities of TMC proteins with these other channels (*4*). Moreover, the pore-forming loop of the channels is located between S5 and S6 (*24*−*26*), whereas our in silico hydropathy analyses imply that any potential pore-forming loop of TMC1 would be located between TM4 and TM5. We, and others, have been unable to directly attribute any channel or transporter activity to TMC1 by electrophysiological methods (unpublished observations and refs *2* and *3*), but its topology justifies continued consideration of this possibility. Finally, the topology of TMC1 provides a foundation for the design and interpretation of experiments that aim to identify interacting protein partners that might give us insight into the possible function of TMC1 and other TMC proteins.

ACKNOWLEDGMENT

We thank our National Institute on Deafness and Other Communication Disorders colleagues for advice and for critical review of the manuscript.

REFERENCES

1. Kurima, K., Peters, L. M., Yang, Y., Riazuddin, S., Ahmed, Z. M., Naz, S., Arnaud, D., Drury, S., Mo, J., Makishima, T., Ghosh, M., Menon, P. S., Deshmukh, D., Oddoux, C., Ostrer, H., Khan, S., Riazuddin, S., Deininger, P. L., Hampton, L. L., Sullivan, S. L., Battey, J. F., Jr., Keats, B. J., Wilcox, E. R., Friedman, T. B., and Griffith, A. J. (2002) Dominant and recessive deafness caused by mutations of a novel gene, TMC1, required for cochlear hair-cell function. *Nat. Genet. 30*, 277–284.
2. Vreugde, S., Erven, A., Kros, C. J., Marcotti, W., Fuchs, H., Kurima, K., Wilcox, E. R., Friedman, T. B., Griffith, A. J., Balling, R., Hrabé de Angelis, M., Avraham, K. B., and Steel, K. P. (2002) Beethoven, a mouse model for dominant, progressive hearing loss DFNA36. *Nat. Genet. 30*, 257–258.
3. Marcotti, W., Erven, A., Johnson, S. L., Steel, K. P., and Kros, C. J. (2006) Tmc1 is necessary for normal functional maturation and survival of inner and outer hair cells in the mouse cochlea. *J. Physiol. 574*, 677–698.
4. Kurima, K., Yang, Y., Sorber, K., and Griffith, A. J. (2003) Characterization of the transmembrane channel-like (TMC) gene family: Functional clues from hearing loss and epidermodysplasia verruciformis. *Genomics 82*, 300–308.
5. Keresztes, G., Mutai, H., and Heller, S. (2003) TMC and EVER genes belong to a larger novel family, the TMC gene family encoding transmembrane proteins. *BMC Genomics 4*, 24.
6. Ramoz, N., Rueda, L. A., Bouadjar, B., Montoya, L. S., Orth, G., and Favre, M. (2002) Mutations in two adjacent novel genes are associated with epidermodysplasia verruciformis. *Nat. Genet. 32*, 579–581.
7. Wilson, I. A., Niman, H. L., Houghten, R. A., Cherenson, A. R., Connolly, M. L., and Lerner, R. A. (1984) The structure of an antigenic determinant in a protein. *Cell 37*, 767–778.
8. Kyte, J., and Doolittle, R. F. (1982) A simple method for displaying the hydropathic character of a protein. *J. Mol. Biol. 157*, 105–132.
9. Choi, B. Y., Stewart, A. K., Madeo, A. C., Pryor, S. P., Lenhard, S., Kittles, R., Eisenman, D., Kim, H. J., Niparko, J., Thomsen, J., Arnos, K. S., Nance, W. E., King, K. A., Zalewski, C. K., Brewer, C. C., Shawker, T., Reynolds, J. C., Butman, J. A., Karniski, L. P., Alper, S. L., and Griffith, A. J. (2009) Hypo-functional SLC26A4 variants associated with nonsyndromic hearing loss and enlargement of the vestibular aqueduct: Genotype-phenotype correlation or coincidental polymorphisms. *Hum. Mutat. 30*, 599–608.
10. Zerangue, N., Schwappach, B., Jan, Y. N., and Jan, L. Y. (1999) A new ER trafficking signal regulates the subunit stoichiometry of plasma membrane K(ATP) channels. *Neuron 22*, 537–548.
11. Margeta-Mitrovic, M., Jan, Y. N., and Jan, Y. L. (2000) A trafficking checkpoint controls GABA(B) receptor heterodimerization. *Neuron 27*, 97–106.
12. Scott, D. B., Blanpied, T. A., Swanson, G. T., Zhang, C., and Ehlers, M. D. (2001) An NMDA receptor ER retention signal regulated by phosphorylation and alternative splicing. *J. Neurosci. 21*, 3063–3072.
13. Plutner, H., Davidson, H. W., Saraste, J., and Balch, W. E. (1992) Morphological analysis of protein transport from the ER to Golgi membranes in digitonin-permeabilized cells: Role of the P58 containing compartment. *J. Cell Biol. 119*, 1097–1116.
14. Wilson, R., Allen, A. J., Oliver, J., Brookman, J. L., High, S., and Bulleid, N. J. (1995) The translocation, folding, assembly and redox-dependent degradation of secretory and membrane proteins in semi-permeabilized mammalian cells. *Biochem. J. 307*, 679–687.
15. Ferguson, P. L., and Flintoff, W. F. (1999) Topological and functional analysis of the human reduced folate carrier by hemagglutinin epitope insertion. *J. Biol. Chem. 274*, 16269–16278.
16. Lin, S., Lu, X., Chang, C. C., and Chang, T. Y. (2003) Human acyl-coenzyme A:cholesterol acyltransferase expressed in Chinese hamster ovary cells: Membrane topology and active site location. *Mol. Biol. Cell 14*, 2447–2460.
17. Krogh, A., Larsson, B., von Heijne, G., and Sonnhammer, E. L. (2001) Predicting transmembrane protein topology with a hidden Markov model: Application to complete genomes. *J. Mol. Biol. 305*, 567–580.
18. Moller, S., Croning, M. D., and Apweiler, R. (2001) Evaluation of methods for the prediction of membrane spanning regions. *Bioinformatics 17*, 646–653.
19. Melen, K., Krogh, A., and von Heijne, G. (2003) Reliability measures for membrane protein topology prediction algorithms. *J. Mol. Biol. 327*, 735–744.
20. Jensen, L. J., Gupta, R., Blom, N., Devos, D., Tamames, J., Kesmir, C., Nielsen, H., Staerfeldt, H. H., Rapacki, K., Workman, C., Andersen, C. A., Knudsen, S., Krogh, A., Valencia, A., and Brunak, S. (2002) Prediction of human protein function from post-translational modifications and localization features. *J. Mol. Biol. 319*, 1257–1265.
21. Jensen, L. J., Gupta, R., Staerfeldt, H. H., and Brunak, S. (2003) Prediction of human protein function according to Gene Ontology categories. *Bioinformatics 19*, 635–642.
22. Kota, J., and Ljungdahl, P. O. (2005) Specialized membrane-localized chaperones prevent aggregation of polytopic proteins in the ER. *J. Cell Biol. 168*, 79–88.
23. Vannier, B., Zhu, X., Brown, D., and Birnbaumer, L. (1998) The membrane topology of human transient receptor potential 3 as inferred from glycosylation-scanning mutagenesis and epitope immunocytochemistry. *J. Biol. Chem. 273*, 8675–8679.
24. Yool, A. J., and Schwarz, T. L. (1991) Alteration of ionic selectivity of a K^+ channel by mutation of the H5 region. *Nature 349*, 700–704.
25. Hartmann, H. A., Kirsch, G. E., Drewe, J. A., Taglialatela, M., Joho, R. H., and Brown, A. M. (1991) Exchange of conduction pathways between two related K^+ channels. *Science 251*, 942–944.
26. Dohke, Y., Oh, Y. S., Ambudkar, I. S., and Turner, R. J. (2004) Biogenesis and topology of the transient receptor potential Ca^{2+} channel TRPC1. *J. Biol. Chem. 279*, 12242–12248.
27. Jones, D. T., Taylor, W. R., and Thornton, J. M. (1994) A model recognition approach to the prediction of all-helical membrane protein structure and topology. *Biochemistry 33*, 3038–3049.
28. Nakai, K., and Horton, P. (1999) PSORT: A program for detecting sorting signals in proteins and predicting their subcellular localization. *Trends Biochem. Sci. 24*, 34–36.
29. von Heijne, G. (1992) Membrane protein structure prediction. Hydrophobicity analysis and the positive-inside rule. *J. Mol. Biol. 225*, 487–494.